Available online at www.sciencedirect.com
ScienceDirect
Applied Catalysis A: General 312 (2006) 134–143
APPLIED CATALYSIS A: GENERAL
www.elsevier.com/locate/apcata

Sol–gel synthesis of V_2O_5–SiO_2 catalyst in the oxidative dehydrogenation of *n*-butane

Viviana Murgia [a,c], Elsa M. Farfán Torres [b,c], Juan C. Gottifredi [a,c], Edgardo L. Sham [a,c,*]

[a] *Facultad de Ingeniería, Universidad Nacional de Salta, Salta, Argentina*
[b] *Facultad de Ciencias Exactas, Universidad Nacional de Salta, Salta, Argentina*
[c] *INIQUI (CONICET), Buenos Aires 177, 4400 Salta, Argentina*

Received 7 December 2005; received in revised form 25 June 2006; accepted 26 June 2006

Abstract

The sol–gel method was used to prepare V–SiO_2 catalyst by hydrolysis of vanadium acetylacetonate and silicon alkoxide. Structural changes in the vanadium species upon heat treatment at various temperatures were studied by means of XRD, XPS; DRS UV–vis, FTIR and FTIR of absorbed pyridine. From characterization studies, it was possible to conclude that during the synthesis process, vanadium acetylacetonate, is adsorbed on the external surface of silica particles formed by tetraethoxysilane hydrolysis. A catalyst prepared by wet impregnation of commercial SiO_2, with identical V/Si surface ratio was used for comparative purposes. The catalytic behaviour of the solids was studied for the oxidative dehydrogenation of *n*-butane. The results indicate that vanadium silicate gel calcined at 500 °C is the most active solid. It was found that this preparation procedure leads to the formation of a solid with a high surface area which allows a better dispersion of active species. A direct correlation between catalytic activity and Brönsted acidity was also observed.

Keywords: Acidity; Butenes; *n*-Butane; Oxidative dehydrogenation; Silica; Sol–gel; Vanadium catalyst

1. Introduction

Catalysts based on supported vanadium oxide exhibit interesting catalytic properties for the partial oxidation of alkanes, aromatics, alcohols and alkenes [1–5]. The activity and selectivity of these catalysts were generally explained on the basis of the nature and distribution of vanadium species, as well as by the vanadium loading and the preparation procedure. The acid–base character of the catalyst also plays an important role [6–9].

The interaction of vanadium oxide with the silica surface is rather low when compared with other supports like alumina and titania [10]. This behaviour was demonstrated by Raman spectroscopy and XANES-EXAFS studies [11,12]. ^{51}V NMR studies also show the presence of V_2O_5 microcrystallites at vanadium loading well below the so-called ''monolayer'' coverage for silica [13]. The sol–gel process was chosen to obtain V–SiO_2 materials with stronger interactions than those observed with impregnated catalysts [1]. The advantages of applying this method to design catalytic materials have already been described in the literature [14,15].

Miller and Lakshmi [16] and Lakshmi et al. [17] have used the sol–gel method to prepare vanadium catalysts supported on TiO_2–SiO_2 and Zr_2O–SiO_2. These catalysts have shown to have a good activity and selectivity in the partial oxidation of ethanol. Vanadium mixed oxide systems, prepared by applying this less conventional technique was tested in the oxidative dehydrogenation of propane [18–20] and ethane [21]. The key point to reach high catalytic performances seems to be the ability to control the nature and interdispersion of the mixed-oxide phases. A preparation method, which causes the vanadium to be distributed homogeneously at the surface and in the bulk, was preferred over a method which deposits vanadium only at the surface [22].

In the present investigation we report the sol–gel synthesis and characterization of vanadia catalysts dispersed on SiO_2 with special emphasis on the acidic properties and the physicochemical characteristics and their correlation with the observed behaviour in the oxidative dehydrogenation of *n*-butane. In order to study the influence of the active phase interaction with the

* Corresponding author. Tel.: +54 387 4255410; fax: +54 387 42510006.
E-mail address: sham@unsa.edu.ar (E.L. Sham).

0926-860X/$ – see front matter © 2006 Elsevier B.V. All rights reserved.
doi:10.1016/j.apcata.2006.06.042

support on the acidic properties developed and the catalytic behaviour, an impregnated catalyst was also prepared and studied.

2. Experimental

2.1. Catalyst preparation

Tetraethoxysilane (TEOS), $Si(OC_2H_5)_4$, and vanadium acetylacetonate ($V(acac)_3$), $V(CH_3COCH{=}COCH_3)_3$, were used as precursors to prepare gels containing 5 wt.% of vanadium.

The preparation was based on a two-step procedure. In the first stage 10 g of VAA were dissolved in methanol (p.a.) and mixed with 100 mL of TEOS under stirring at room temperature. The clear green solution formed was refluxed for 2 h. Then 10 mL of water and 10 mL of ammonium hydroxide (25 wt.%) were added to allow the formation of a gel. The final product was washed with water and dried at 60 °C to obtain a fine yellow powder.

Then, the solid was calcined at 500, 600 and 700 °C over 16 h. The materials prepared were identified as SiVa-*x* °C, where *x* °C is the calcination temperature. A fraction of the gel was also activated with another procedure. The solid was suddenly heated at 700 °C for a short period of time and then calcined like the others at 500 °C. It was identified as SiVa-TS (TS stands for thermic shock).

A reference catalyst with the same V/Si surface ratio was prepared by wet impregnation of silica (Aldrich, 216 $m^2\ g^{-1}$) with ammonium methavanadate solutions. This solid had a vanadium content of 1.4 wt.% and was named $V1.4/SiO_2$. This catalyst was also dried at 60 °C and calcined for 16 h at 500 °C.

2.2. Catalyst characterization

X-ray diffraction (XRD) patterns were collected in a Rigaku diffractometer D_{max}-IIC using Cu Kα radiation (λ = 0.1549 nm).

Diffuse reflectance spectra (DR) in the UV–vis region were obtained with a GBC-UV/Vis 918 equipped with an integer sphere and using $BaSO_4$ as blank reference.

Infrared spectra were recorded between 2000 and 400 cm^{-1} with a Bruker IFS 88 on samples dispersed in KBr and pressed in thin wafers.

Acidity was studied by FTIR of adsorbed pyridine on self-supported thin wafers. The analysed range was 2000–400 cm^{-1}. Samples were previously evacuated at 250 °C for 1 h. Then pyridine was adsorbed followed by evacuation for 30 min at room temperature, 100 and 150 °C. In some cases after this treatment water vapour was adsorbed at room temperature. For SiVa-500 °C and SiVa-TS a pretreatment evacuation temperature of 450 °C was also used.

The XPS spectra were taken in a Physical 5700 ESCA spectrometer. The exciting radiation was Mg Kα (1253.6 eV). The binding energies (BE) were calculated with respect to C1s peak set at 284.5 eV. The chemical composition of samples were determined by atomic absorption spectrometry using a GBC 904AA, equipped with a Vanadium lamp at λ = 318.3 nm. Samples were digested with a mixture of HF and H_2SO_4.

Thermogravimetric and differential thermal analysis (ATD-TG) were performed on a Rigaku TAS 1000, heating the samples in air with a heating speed of 10 °C min^{-1} from room temperature up to 1000 °C.

Raman spectroscopy was performed with a DILOR-JOBIN YVON-SPEX spectrometer model OLYMPUS DX-40, equipped with a He–Ne (λ = 632.8 nm) laser. The spectral resolution was 7 cm^{-1}, and the spectra acquisition consisted of three accumulations of 30 s for each sample.

2.3. Catalytic tests

n-Butane oxydehydrogenation (ODH) was studied in an isothermal stainless steel microreactor fed with a mixture of 15/20/65 of oxygen, *n*-butane and nitrogen, respectively, at a constant rate of 150 mL min^{-1}. A constant amount of catalyst (0.4 g, particle sizes between 150 and 250 μm) was diluted in quartz. The reaction temperature range varied between 400 and 600 °C to achieve different conversion levels. Blank tests on the same reactor showed no activity in all range of temperatures studied.

Reactants and reaction products were analysed by means of two on-line chromatographers, Shimatzu GBC- and Varian 3700.

3. Results

The surface area and vanadium content are given in Table 1. XRD patterns of SiVa catalysts are presented in Fig. 1.

Table 1
Characteristics of supported vanadium catalysts

Catalyst	S_g ($m^2\ g^{-1}$)	Vanadium content (%)
SiVa-60 °C	273.4	4.02
SiVa-500 °C	475.8	4.57
SiVa-600 °C	160.5	5.04
SiVa-700 °C	90.5	5.02
SiVa-TS	430.8	4.56
$V1.4/SiO_2$	260.2	1.20
SiO_2	216.1	–

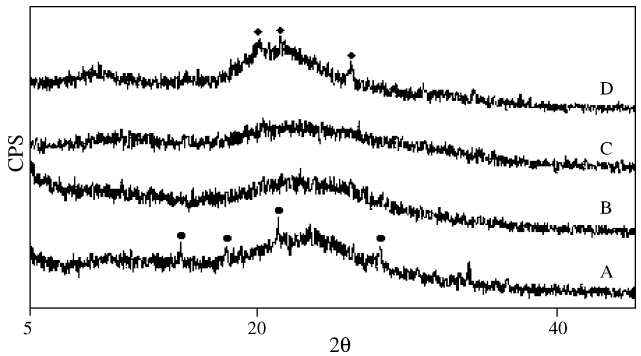

Fig. 1. DRX patterns of SiVa: (A) SiVa-60 °C; (B) SiVa-500 °C; (C) SiVa-600 °C; (D) SiVa-700 °C. ◆, V_2O_5; ●, vanadate species.

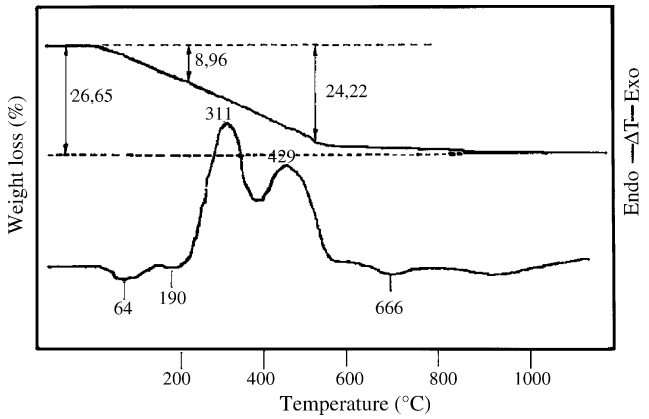

Fig. 2. ATD-TG SiVa–60 °C.

In the case of the gel dried at 60 °C (curve A), four low intensity diffraction lines at 5.909, 4.930, 3.783 and 3.175 Å were observed. These lines correspond to vanadium species with crystalline structure of vanadate type. SiVa-500 °C and SiVa-600 °C show pattern characteristic of amorphous silica. In the case of SiVa-700 °C very low diffraction lines at 4.427, 4.153 and 3.417 Å, corresponding to the formation of V_2O_5 microcrystallites were detected.

Differential thermoanalysis as well as mass losses were recorded for SiVa-60 °C and are presented in Fig. 2.

Two broad endothermic events around 64 and 190 °C occurred due to the removal of adsorbed water and ammonium residual groups. These events were related to a mass loss of about 9% of initial weight. For higher temperatures, two exothermic transformations that reach their maximum at 311 and 429 °C were observed and were assigned to the removal of two acetylacetonate groups grafted on the silica surface, related to a mass loss of 15.2%. Another endothermic event at 666 °C not associated with a mass loss was detected. It can be related to a crystalline structural change.

DR UV–vis spectra of SiVa catalysts are presented in Fig. 3. Bands related to tetrahedral and octahedral species were observed for all the solids. The octahedral species were related with V^{5+} ions which present characteristic absorption bands between 350 and 500 nm. While, highly dispersed tetrahedral species of V^{4+} and V^{5+} could be related to contributions between 240–280 nm and 280–340 nm, respectively [8,23–25].

SiVa-500 °C spectrum, Fig. 3B, shows a broad absorption band with a maximum at 265.0 and 389.3 nm, corresponding to vanadium ions in tetrahedrical and octahedrical coordination, respectively.

When the calcination temperature increases up to 600 °C, the presence of a unique band at 280.0 nm shows that isolated tetrahedral species VO_x were predominant in this case (Fig. 3C). For SiVa-700 °C, more definite bands were observed, corresponding to tetrahedral (240 nm) and octahedral coordination ions (380 nm).

SiVa-TS (Fig. 3E) exhibits a spectrum similar to SiVa-500 °C, although an increase in tetrahedral species is observed.

DR UV–vis spectra of SiO_2 and V1.4/SiO_2 catalysts are presented in Fig. 4. Before calcination, a broad band between 350 and 500 nm indicates that both forms of vanadium coordination ions were present on the surface of this solid. After calcination, V1.4/SiO_2 spectrum is like SiVa-500 °C.

Infrared spectra of SiVa materials in the 2000–400 cm^{-1} region are reproduced in Fig. 5. For SiVa-60 °C (Fig. 5A) the following absorption bands are observed: 1639 cm^{-1} attributed to physisorbed water; 1400 and 669 cm^{-1} corresponding to residual ammonia; 1080 and the shoulder at 1216 cm^{-1} assigned to asymmetric stretching vibrations of the three-dimensional Si–O–Si network; 958 cm^{-1} due to the presence of surface Si–O^- groups in silica gels; 800 cm^{-1} attributed to symmetric stretching vibration of the Si–O–Si network and 459 cm^{-1} assigned to Si–O–Si bending deformation [26,27].

After heat pretreatment the band corresponding to Si–O–Si vibrations becomes narrow and shifts to 1082, 1103 and 1107 cm^{-1} for SiVa-500 °C, SiVa-600 °C and SiVa-700 °C, respectively.

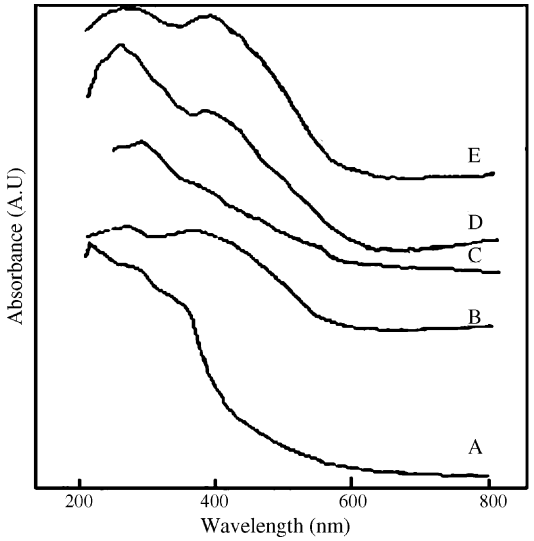

Fig. 3. DR UV–vis: (A) SiVa-60 °C; (B) SiVa-500 °C; (C) SiVa-600 °C; (D) SiVa-700 °C; (E) SiVa-TS.

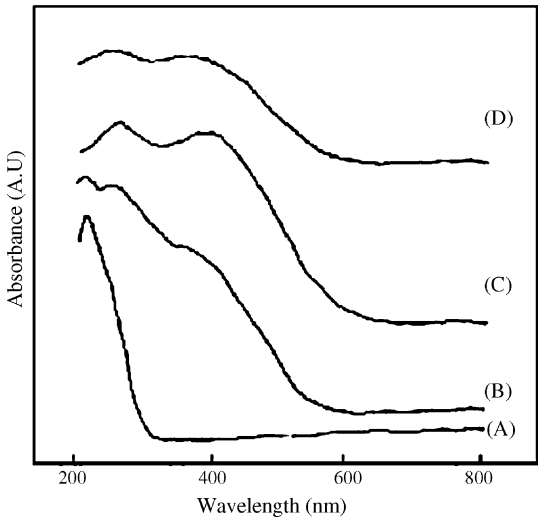

Fig. 4. DR UV–vis: (A) SiO_2; (B) V1.4/SiO_2-60 °C; (C) V1.4/SiO_2-500 °C; (D) SiVa-500 °C.

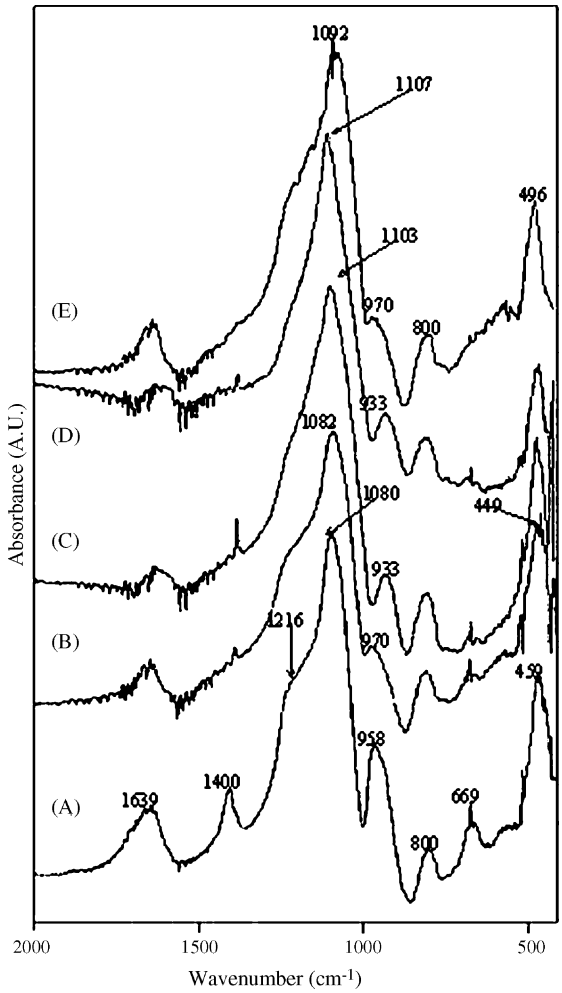

Fig. 5. IR spectra: (A) SiVa-60 °C; (B) SiVa-500 °C; (C) SiVa-600 °C; (D) SiVa-700 °C; (E) SiVa-TS.

The band at 958 cm^{-1} was also very sensible to heat treatment, losing intensity and shifting to 970 cm^{-1} for SiVa-500 °C.

In the literature bands at 980 cm^{-1} were related to vibration of Si–O–H groups [28]. This band was also correlated to asymmetric stretching mode of SiO_4 tetrahedrons connected to V-ions. This band was found at 960 cm^{-1} for V-silicalites [29] and at about 950 cm^{-1} for vanadia–silica xerogels [30]. In other works the band at 930 cm^{-1} was assigned to a Si–O–V stretch mode, and it is also postulated that both Si–O–V and V–O–V bridges can contribute to this band [31]. In the case of SiVa materials silanol vibrations are probably superimposed to the Si–O–V stretching modes. For high calcination temperatures (Fig. 5C and D) a Si–O–V absorption band is observed at 933 cm^{-1}.

Band intensity corresponding to residual ammonia 1400 and 669 cm^{-1} decreases with the calcination temperature being completely absent for SiVa-700 °C (Fig. 5D).

The IR spectrum of SiVa-TS catalyst was similar to that of SiVa-500 °C. The γ-Si–O–Si vibration mode shifted to 1092 cm^{-1} and residual ammonia band was completely absent.

The IR spectra of SiO_2 and V1.4/SiO_2 are shown in Fig. 6A and B, respectively. Both spectra are very similar. Only a slight

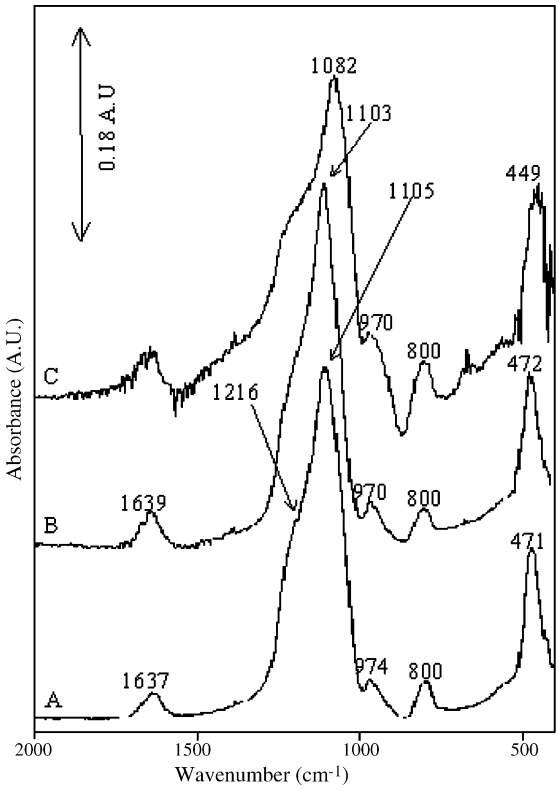

Fig. 6. IR spectra: (A) SiO_2; (B) V1.4/SiO_2; (C) SiVa-500 °C.

shift to lower wavenumbers due to weak interaction of vanadia with the silica support is observed.

The Si–O–V stretching bands cannot be detected due to a possible overlapping with the silanols groups of SiO_2.

The binding energies and V/Si atomic ratios determined from XPS are presented in Table 2.

The low BE values observed for SiVa-60 °C suggest that species like VO^+ could be present in dried gels before calcination [32]. When SiVa gels are calcined, the BE values correspond predominantly to V^{4+} species in all the cases. Similar values of BE were observed for impregnation catalysts. Only SiVa-700 °C has a BE related to a bigger fraction of V^{5+} species. The BE corresponding to Si 2p levels indicate the presence of chain of silicates for SiVa-60 °C [32]. After calcination, the BE characteristics of silica gel were found for all the solids studied.

Table 2
Binding energies and V/Si atomic ratios for SiVa and V1.4/SiO_2 catalysts

Catalyst	BE (eV)		Surface atomic ratio, V/Si
	V $2p_{3/2}$	Si 2p	
SiVa-60 °C	515.50	102.60	0.38
SiVa-500 °C	516.30	103.12	0.048
SiVa-600 °C	516.20	103.10	0.054
SiVa-700 °C	516.70	103.00	0.066
SiVa-TS	516.40	103.25	0.050
V1.4SiO_2/60 °C	516.40	102.50	0.057
V1.4SiO_2/500 °C	516.20	102.80	0.050

The atomic ratios V/Si can be taken as a relative measure of vanadium dispersion on the SiO_2 [33], and were determined from the integral of the signal corresponding to V $2p_{3/2}$ and Si 2p. SiVa-60 °C gel shows a high vanadium surface concentration indicating vanadium species were essentially dispersed on the silica particles formed by hydrolysis.

When solids were calcined at 500 °C, V/Si ratio strongly decreased. Then, as calcination temperature increases, V/Si ratio also increases, showing reorganization in the solid. SiVa-700 °C presents the highest value for this ratio, which is consistent with the lost of superficial area produced by dehydration of the SiO_2 network. At the same time the surface vanadium oxide collapses and sinters forming small crystalline V_2O_5 particles shown by the XRD at 700 °C.

It is noticeable that V1.4/SiO_2 and SiVa-500 °C show a very similar superficial ratio V/Si.

In Fig. 7 the infrared spectra of pyridine adsorbed on SiVa-500 °C after evacuation at different temperatures are presented.

Spectrum (a) shows bands at 1597 and 1446 cm^{-1} corresponding to 8a and 19b modes of pyridine species linked through hydrogen bonds. Characteristic bands of pyridine retained on Lewis acid sites at 1608, 1579, 1489 and 1446 cm^{-1} were observed [25,34]. Peaks at 1639 and 1544 cm^{-1}, associated with pyridine adsorbed on Brönsted acid sites, were also present. After evacuation at 100 °C (spectrum b), the bands associated with hydrogen bonds were removed and shifted from 1446 to 1450 cm^{-1} and from 1608 to 1610 cm^{-1}. Pyridine species bonded to both types of acid sites have low intensity after evacuation at 150 °C. For all catalysts spectra present bands related to Brönsted and Lewis acid sites.

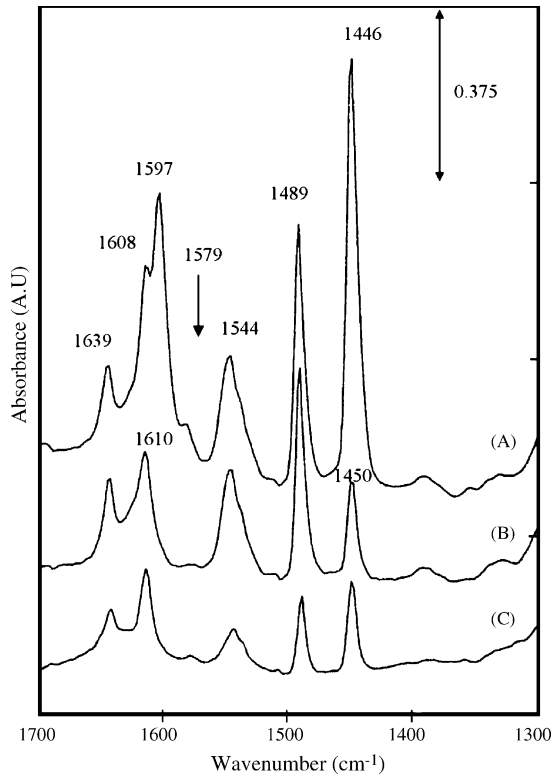

Fig. 7. FTIR spectra of pyridine adsorbed on SiVa-500 °C. Pretreatment: 1 h 250 °C: (A) after evacuation 30 min RT; (B) after evacuation 30 min RT + 30 min 100 °C; (C) after evacuation 30 min RT + 30 min 100 °C + 30 min 150 °C.

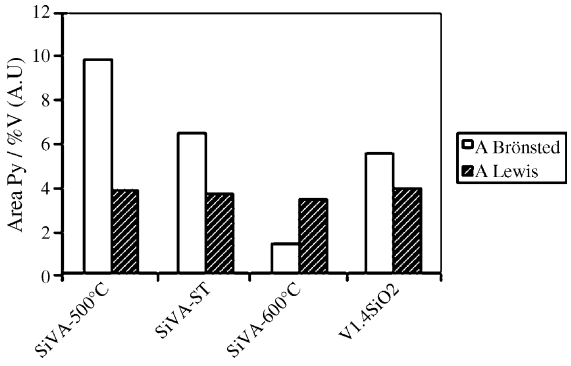

Fig. 8. Pyridine adsorption for SiVa and V1.4/SiO_2.

By integrating the band at 1544 cm^{-1} the area corresponding to Brönsted acid sites can be obtained. With the same procedure with bands at 1450 cm^{-1} the area belonging to Lewis acid sites is estimated. Fig. 8 illustrates these results, expressed as pyridine area normalized with respect to vanadium content of catalysts.

As it can be seen, the total acidity decreases according to the following trend: SiVa-500 °C > SiVa-TS > V1.4/SiO_2 > SiVa-600 °C. It was noticeable that the normalized Lewis area is the same in all the cases, while normalized Brönsted area changes notably for the different solids. Additional tests were carried out for SiVa-500 °C and V1.4/SiO_2, using a pretreatment temperature of 450 °C. These results are shown in Fig. 9.

The same trend is observed for these solids. The total acidity of SiVa-500 °C is greater than that observed for V1.4/SiO_2. An increase in the acid Lewis sites that can be correlated with a decrease in the Brönsted area is observed. This fact shows that under vacuum calcination conditions, dehydroxylation processes take place, exchanging these acid sites to each other.

Another test was conducted consisting of addition of water vapour on SiVa-500 °C, after pretreatment at 450 °C.

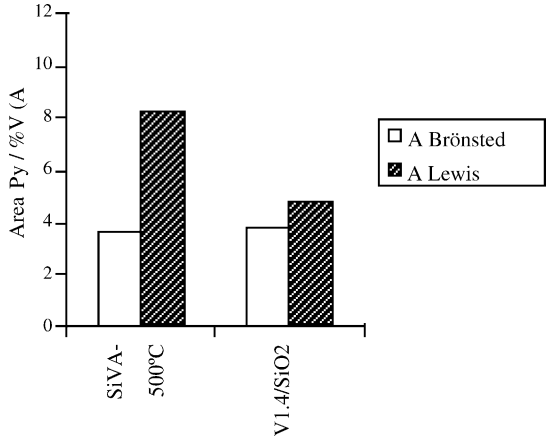

Fig. 9. Pyridine adsorption for SiVa and V1.4/SiO_2.

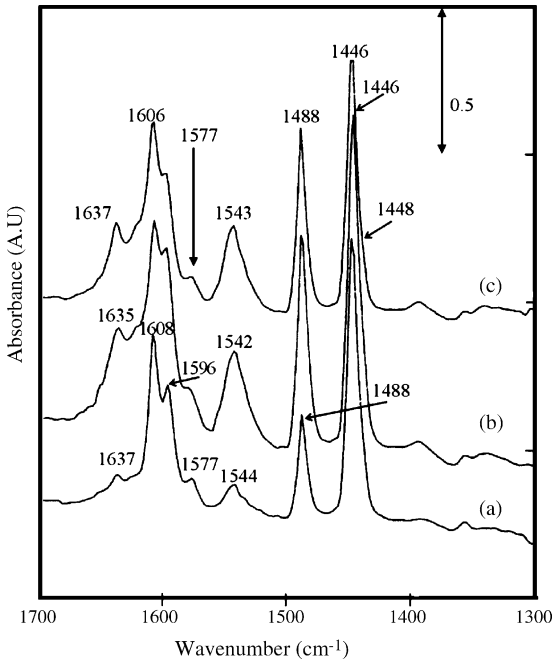

Fig. 10. Adsorption pyridine spectrum at RT and later adsorption of H_2O + pyridine. (a) Pyridine adsorption and later evacuation 30 min at RT; (b) H_2O + pyridine adsorption and later evacuation 5 min at RT; (c) H_2O + pyridine adsorption and later evacuation 30 min at RT.

This experiment was carried out by means of pyridine adsorption at room temperature with a later evacuation for 30 min at RT. In Fig. 10 (spectrum a) it can be observed that the ratio of Brönsted to Lewis acid sites is low. Then, a pulse of water vapour and pyridine was added. After that, evacuations during 5 and 30 min at RT were performed. A complete regeneration of Brönsted sites occurred, as can be seen in Fig. 10 (spectrum b and c).

The Raman spectra of V_2O_5 and SiVa-*x* °C are shown in Fig. 11. A sharp band at 1040 cm^{-1} was observed for SiVa-500 °C, which has been assigned to the stretching mode of the terminal V=O bond, arising from isolated VO_4 species [39–41].

The absence of the band at 775 cm^{-1} assignable to symmetric stretching modes of V–O–V polyvanadates species,

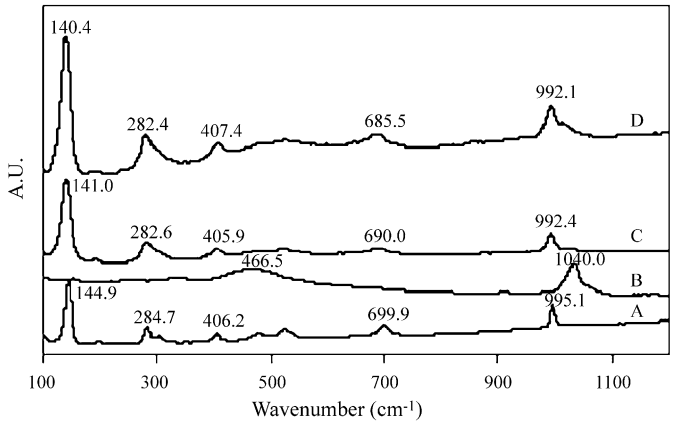

Fig. 11. Raman Spectra: (A) V_2O_5; (B) SiVA-500 °C; (C) SiVA-600 °C; (D) SiVA-700 °C.

confirms that only monovadate groups are present for this solid. The broad band centred at 467 cm^{-1} was also observed for SiVa-500 °C. This band corresponds to cyclic siloxanes groups [39].

For SiVa-600 °C and SiVa-700 °C, a well-defined band appears at near 144 cm^{-1}, which is assignable to the formation of crystalline V_2O_5. The spectra of these samples also show bands at 992, 690, 406, 283 and 141 cm^{-1} arising from V_2O_5 crytallites.

3.1. Oxidative dehydrogenation of n-butane

Table 3 shows conversion of *n*-butane (XC_4) and oxygen (XO_2) and the distribution of reaction products, obtained at each temperature. The predominant reaction products were dehydrogenation products (1-butene, trans and *cis*-2-butene and 1,3-butadiene) and carbon oxides, while cracking products were minor or absent.

It can be seen that, conversion levels are significantly higher on SiVa-500 °C and SiVa-TS. The latter presents lower selectivity than SiVa-500 °C; while SiVa-600 °C and SiVa-700 °C have the lowest selectivity to ODH products.

In Fig. 12 yields to ODH reaction products for all the solids studied are presented. At the same reaction temperature V1.4/SiO_2 was the most selective solid, but it is less active than SiVa-500 °C. Thus, a higher yield was reached by SiVa-500 °C.

Although V1.4/SiO_2 was shown as the most selective catalyst at each temperature, conversion was always smaller compared with SiVa-500 °C Since the reaction scheme involves consecutive reactions an increase in selectivity with low conversion is to be expected. The highest yields were observed with SiVa-500 °C and SiVA-TS at temperatures ranging from 562 to 584 °C.

In every case the predominant product of the oxydehydrogenation was 1-butene while butadiene selectivity increased with temperature. At very low temperatures, the only observed reaction product was CO_2.

In Table 4, initial reaction rates (calculated at conversion below 10%) are presented.

Again, it is clearly shown that vanadium was more active on SiVa-500 °C and SiVa-TS than on impregnated catalysts.

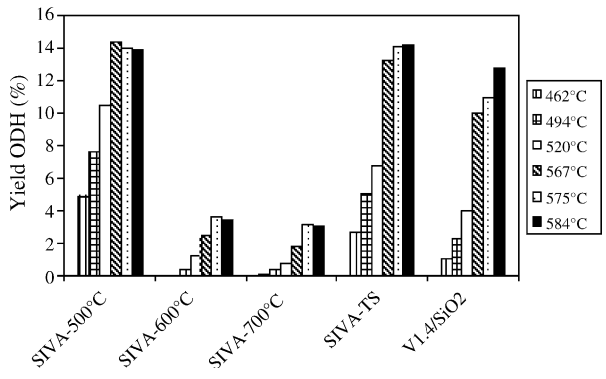

Fig. 12. Yield to ODH reaction products (%).

Table 3
ODH of *n*-butane: SiVa and V1.4/SiO_2

T (°C)	Catalyst	X_{C_4}	X_{O_4}	$S_{C_4H_8}$	$S_{C_4H_6}$	S_{COMB}	S_{CRAQ}
462	V1.4/SiO_2	1.29	3.78	78.5	–	21.50	–
	SiVa-500 °C	9.29	54.17	47.3	5.28	47.26	0.36
	SiVa-TS	7.46	42.75	34.91	–	65.08	–
	SiVa-600 °C	1.71	13.87	–	–	100.00	–
	SiVa-700 °C	1.53	14.63	5.09	–	94.90	–
494	V1.4/SiO_2	2.87	12.17	70.19	6.48	23.34	–
	SiVa-500 °C	17.28	96.43	36.81	7.35	54.70	1.14
	SiVa-TS	15.49	79.39	28.91	3.74	66.06	1.29
	SiVa-600 °C	5.39	35.75	7.26	–	92.74	–
	SiVa-700 °C	2.77	25.22	12.25	–	87.85	–
520	V1.4/SiO_2	5.54	12.67	63.75	8.75	27.59	–
	SiVa-500 °C	21.01	99.55	37.92	11.6	48.28	2.20
	SiVa-TS	19.61	96.03	29.26	5.13	63.97	1.64
	SiVa-600 °C	9.23	55.86	12.76	–	86.26	0.98
	SIVa-700 °C	5.78	40.04	12.17	–	86.88	0.95
566	V1.4/SiO_2	15.53	46.34	51.65	12.85	32.67	2.83
	SiVa-500 °C	26.29	99.56	38.89	15.64	40.74	4.72
	SiVa-TS	27.07	99.62	36.23	12.44	47.63	3.70
	SiVa-600 °C	16.43	91.49	13.21	1.48	83.55	1.77
	SiVa-700 °C	11.63	68.22	15.33	–	82.09	2.38
575	V1.4/SiO_2	17.16	49.56	49.75	14.11	32.84	3.29
	SiVa-500 °C	26.01	99.55	38.55	15.19	41.55	4.71
	SiVa-TS	28.11	99.62	36.56	13.56	46.05	3.83
	SiVa-600 °C	17.93	94.96	18.08	2.32	77.70	1.89
	SiVa-700 °C	12.71	74.46	22.29	2.08	73.15	2.49

$C_4/O_2/N_2$: 20/15/65; Q_T = 150 mL min^{-1}; W/F = 6.26 g_{cat} per h mol C_4; X: conversion; S: selectivity.

Table 4
Reaction rate, R_v

Catalyst	T (°C)	X_{C_4} (%)	R_v (mol C_4 (h mol V)$^{-1}$)	S_{ODH} (%)
SiVa-500 °C	462	9.29	16.54	52.28
SiVa-TS	462	7.46	13.28	34.91
SiVa-600 °C	462	1.71	2.76	–
	494	5.39	8.70	7.26
	520	9.23	14.90	12.76
SiVa-700 °C	462	1.53	2.47	5.09
	494	2.77	4.47	12.25
	520	5.78	9.33	12.17
V1.4/SiO_2	462	1.29	8.75	78.50
	490	2.87	19.46	76.66
	520	5.54	37.57	72.40

$C_4/O_2/N_2$: 20/15/65; Q_T = 150 mL min^{-1}; W/F = 6.26 g_{cat} per h mol C_4.

4. Discussion

4.1. Characterization studies

From chemical analyses, DRX, ATD-TG, FTIR and XPS, it is possible to conclude that during the synthesis process, vanadium acetylacetonate, $V(acac)_3$, is adsorbed on the external surface of silica particles formed by tetraethoxysilane hydrolysis. The interchange mechanism involves loss of one acetylacetonate group of $V(acac)_3$ coordination sphere, while one Si–O–H group is incorporated:

$$Si{-}OH + V(acac)_3 \rightarrow Si{-}O{-}V(acac)_2 + H(acac)$$

This acetylacetonate ligand is not readsorbed on silica surface, since compounds like Si(acac) are extremely unstable and the formation of this species is very improbable [31].

From IR spectrum it can be observed that the absorption band corresponding to ν-Si–O–H, whose normal absorption takes place at 975 cm^{-1} (for highly ordered dehydrated silica) is strongly shifted to 958 cm^{-1} for SiVa-60 °C. This shifting can be related to the substitution of vanadium by hydrogen in the silanol groups, as it is reported in the case of deuteration of this groups [35]. This fact supports the proposed mechanism.

XPS and XRD also confirm this mechanism, since the BE energies of V $2p_{3/2}$ level provides a strong indication of the presence of VO^+ species. In other words vanadium species do not change their oxidation state during the adsorption. BE values for Si 2p are due to tetramers of SiO_2. So, SiVa-60 °C catalysts are essentially formed by highly hydrated silica on the external surface of which vanadium acetylacetonate [III] is exchanged. As indicated by high V/Si atomic ratios (Table 2). IR absorption bands at 1080 and 1216 cm^{-1} show that well organized tetrahedron silica network is formed.

SiVa-500 °C IR shows a slight shift of ν-Si–O–Si to 1082 cm^{-1}, but a band shift at 970 cm^{-1} confirms that, at this temperature, a solid state reaction takes place. At the same time,

in agreement with chemical analysis and ATD-TG studies, two acetylacetonate ligands bonded to vanadium species adsorbed on the surface, are lost. When this occurs, tetrahedric amorphous species are formed, as confirmed by the disappearance of diffraction lines in the diffractograms (Fig. 1B). The presence of the characteristic band at 1040 cm^{-1} in the Raman spectra shows that these tetrahedric species correspond to V=O bonds in terminal monovanadate isolated groups.

From these findings a mechanism for the process taking place from V[acac]$_3$ exchange to calcination at 500 °C can be suggested. At the same time, it involves, a structure rearrangement that changes vanadium distribution over silica and dispersion into the bulk network, as can be noted by the decrease of V/Si ratio. In Scheme 1, the proposed mechanism is presented. Agglomeration of silica would also encapsulate the vanadia clusters, thereby decreasing the surface V/Si ratio.

For SiVa-500 °C, SiVa-600 °C and SiVa-700 °C the band at 1080 cm^{-1} shifts to higher wavenumbers. This shift was observed by other authors as a result of increased temperature treatments for silica gels [26]. It was proposed that it reflects an increased rigidity of the Si–O–Si network when condensation occurs. For SiVa-600 °C and SiVa-700 °C, the band belonging to ν-Si–O–Si becomes more intense and narrow and shifts to higher wavenumbers values (1103–1107 cm^{-1}). The observed increase in the definition and intensity of this band is produced when water is released from the SiO_2 network as the Si–O–H groups are changed to Si–O–Si groups. These results show that silica network developed by the sol–gel process is in fact well organized. For these solids it is also observed that the band at 970 cm^{-1} shifts to 933 cm^{-1}. As in these solids the dehydration degree is strong, there is no more contribution of silanol groups to the absorption as was confirmed by the Si–O–Si band shape, and then this absorption frequency corresponds to Si–O–V species [30,31].

SiVa-TS catalysts show a very similar structure and vanadium dispersion as SiVa-500 °C. DR-UV–vis spectra exhibit that the most important difference between these materials is the hydration degree which appears to be lower in SiVa-TS. Probably the short heat treatment at 700 °C produces a larger fraction of tetrahedral species. Recent works suggest that part of the tetrahedral surface species that interact with water molecules forms a distorted octahedral coordination environment after water adsorption [36,37].

From DR-UV–vis and IR results the presence of tetrahedral and octahedral species was confirmed in the V1.4/SiO_2 catalyst. Even at very low vanadium content the formation of bulk

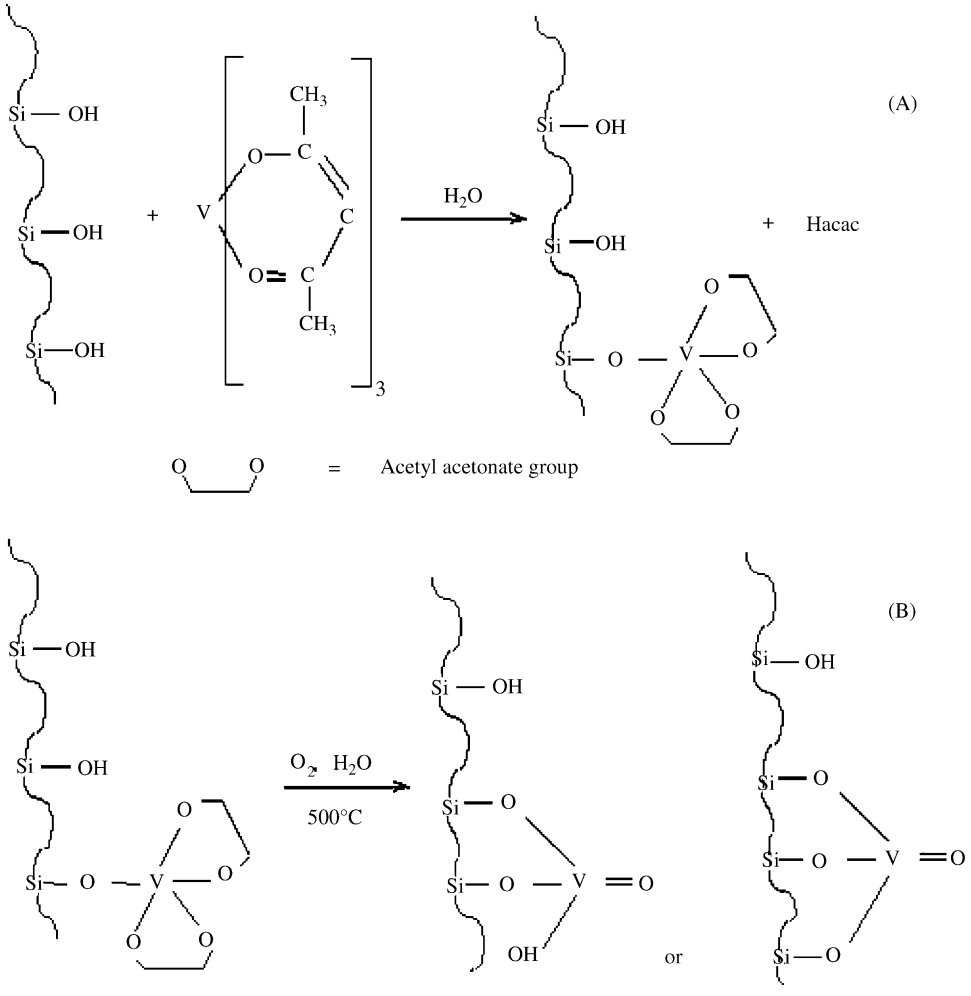

Scheme 1. General reaction mechanisms for the synthesis of the SiVa catalyst: (A) after V(acac)$_3$ exchange; (B) after calcination at 500 °C.

species have also been proposed in the literature [13] for catalyst prepared by impregnation of SiO_2.

From XPS, DR-UV–vis and IR studies it is possible to conclude that SiVa-500 °C and V1.4/SiO_2 present almost the same vanadium surface dispersion and have a similar structure. We must remark that these solids present an important difference in surface area, as should be expected with the preparation procedure used here. The high surface area developed by the sol–gel process permits to obtain the same dispersion for a higher vanadium content.

Pyridine adsorption studies indicate a large amount of Brönsted acid sites on SiVa-500 °C. One model used to explain the generation of these sites, is that the electron density of an OH bond is reduced by the inductive effects of the nearby electronegative anions, weakens this bond and thus generates a Brönsted site. So the presence of this type of sites could be related, on one hand to the presence of electronegative anions and on the other hand to a high silanol density neighbour [38]. This different capacity to generate acid types shows that the hydration degree between the SiO_2 network obtained from the sol–gel synthesis and the commercial silica is the main difference between both catalysts.

4.2. Catalytic studies

As stated above the presence of CO_2, as the initial reaction product, detected in this reaction system as temperature was increased clearly suggest a competitive parallel mechanism to account for *n*-butane conversion. As a consequence *n*-butane can be straight forwardly converted to CO and CO_2 or to dehydrogenated compounds which can also reacts with similar parallel mechanism to produce carbon oxides or further dehydrogenated products. A remarkable result is the continuous decrease of ODH selectivity as conversion increased as observed for V1.4/SiO_2. However this is not the case for SiVa-500 °C and SiVa-TS since first selectivity decreases with conversion but remains constant or shows a tendency to increase when conversion is higher that 18%. This behaviour must be related to the almost whole O_2 conversion (see Table 3) observed at this stage suggesting more favourable conditions for dehydrogenated products under such limiting conditions [42]. Thus, the highest yields are observed at the highest temperature investigated since the limiting O_2 conditions are met.

It is noticeable that using 15/20/65 oxygen, *n*-butane and nitrogen feed, the catalysts which had developed the highest conversion levels can keep or improve the ODH selectivity by oxygen consumption control. This observation confirms that catalytic behaviour is influenced by the solid structure as well as by reaction condition. For SiVa-500 °C cracking products were observed even at low reaction temperatures and selectivity to these products becomes significant at higher temperatures. This catalyst presents the highest cracking selectivities as well as the highest Brönsted acid site content observed.

SiVa-600 °C and SiVa-700 °C were less active and presented low selectivity to ODH as can be observed since *n*-butane conversion was always below 18% although O_2 was completely converted. Thus these catalysts favor *n*-butane direct oxidation to carbon oxides. SiVa-600 °C and SiVa-700 °C also show vanadium dispersion and surface areas lower than SiVa-500 °C. Consequently these also explain the activity and selectivity results. As discussed previously high calcination temperatures could lead toV_2O_5 microcrystallites formation and sintering phenomena that could deactivate active reaction centers.

A direct correlation between catalytic activity (mol C_4 (mol V h)$^{-1}$) and Brönsted acidity (%Area Py (mol V)$^{-1}$) can be established from Table 4 and Fig. 8. In actual facts these two variables show the same tendency: SiVa-500 °C > SiVa-TS > V1.4/SiO_2 > SiVa-600 °C, while Lewis acidity is the same for all the solids. It can be concluded that Brönsted acid sites have a direct influence on catalytic activity. It should also be noticed that water is a reaction product and that, as shown in Fig. 10, surface rehydroxilation favors the formation of Brönsted sites which ensures the permanent presence of them throughout the reaction experiments.

Results reported by Le Bars et al. [6] in the ODH ethane reaction are in agreement with this correlation and showed the existence of a linear relation between conversion rate of ethane and acid surface character of V/SiO_2 catalyst. These authors also report that an increase in the acidity of vanadium oxides dispersed on SiO_2 improved the ethane to ethene ODH rate, although this increase in the acidic character is not accompanied by an increase in selectivity.

In our work similar results are found for selectivity. The most active catalysts which were the more acidic were not the most selective. The impregnated catalyst, which shows an intermediate acidity, with a lower amount of Brönsted acid sites, has higher values of selectivity, but at lower conversion levels (see Table 3).

5. Conclusions

The hydrolytic sol–gel method was adopted in this work to prepare V–SiO_2 solids. It can be a potential procedure to prepare active ODH catalyst.

The analytical, spectroscopic and chemical results show that during the synthesis process an exchange mechanism takes place, involving the loss of one acetylacetonate group from $V(acac)_3$ which is incorporated at one Si–O–H group.

After heat treatment the solid structure is rearranged conducting to the formation of VO_x species homogeneously dispersed in the SiO_2 network.

Our results show that vanadium–silica catalysts prepared by the sol–gel method were active catalysts for the oxidative dehydrogenation of *n*-butane. This catalyst calcined at 500 °C was more active than the impregnated one having the same surface vanadium dispersion.

Differences in activity were attributed to the development of a hydrated vanadia silica phase which favors the Brönsted acid sites formation. The main structural difference between the sol and gel catalyst and the impregnated one is the development of a high surface area for the first one, which allows a better dispersion of active species.

The catalytic behavior of a sol–gel material is quite similar to that observed for a V/Al_2O_3 catalyst [42]. When calcination temperature increases, the dispersion, specific surface and hydration degree decrease together with the catalytic activity and selectivity.

Acknowledgement

Financial support by CONICET from Argentina, PIP 02821, is gratefully acknowledged.

References

[1] E.L. Sham, V. Murgia, J.C. Gottifredi, E.M. Farfán Torres, in: B. Delmon, et al. (Eds.), Preparation of Catalysis VII, Elsevier Science B.V., Amsterdam, 1998, pp. 669–678.
[2] E.A. Mamedov, V. Cortés Corberán, Appl. Catal. A: Gen. 127 (1995) 1–40.
[3] B.M. Weckhuyen, D.E. Keller, Catal. Today 78 (2003) 25–46.
[4] B. Solsona, A. Dejoz, M.I. Vazquez, F. Márquez, J.M. López Nieto, Appl. Catal. A: Gen. 208 (2001) 99–110.
[5] A. Bottino, G. Capannelli, A. Comite, S. Storace, R. Di Felice, Chem. Eng. J. 94 (2003) 11–18.
[6] J. Le Bars, J.C. Vedrine, A. Auroux, Appl. Catal. A: Gen. 88 (1992) 179–195.
[7] T. Blasco, J.M. López Nieto, A. Dejoz, M.I. Vázquez, J. Catal. 157 (1995) 271–282.
[8] T. Blasco, A. Galli, J.M. López Nieto, F. Trifiró, J. Catal. 169 (1997) 203–211.
[9] M. Machli, E. Heracleous, A.A. Lemonidou, Appl. Catal. A: Gen. 236 (2002) 23–34.
[10] R. Kozlowski, R. Pettifer, J.M. Thomas, J. Phys. Chem. 87 (1983) 5176–5181.
[11] F. Roozeboom, M.C. Mittelmejeir-Hazeleger, J.A. Moulijn, J. Medema, V.H.J. de Beer, P. Gellings, J. Phys. Chem. 84 (1980) 2783–2791.
[12] J. Haber, A. Kozlowska, R. Kozlowski, J. Catal. 102 (1986) 52–63.
[13] M.M. Koranne, J.G. Goodwin, G. Marcelin, J. Catal. 148 (1994) 369–377.
[14] M.A. Cauqui, J.M. Rodriguez Izquierdo, J. Non-Cryst. Solids 147/148 (1992) 724–738.
[15] G.M. Pajonk, Appl. Catal. 72 (1991) 217–266.
[16] J.M. Miller, J.L. Lakshmi, J. Catal. 184 (1999) 68–76.
[17] J.L. Lakshmi, N.J. Ihasz, J.M. Miller, J. Mol. Catal. A: Chem. 165 (2001) 199–209.
[18] O.R. Evans, A.T. Bell, T. Don Tilley, J. Catal. 226 (2004) 292–300.
[19] J.D. Pless, B.B. Bardin, H.S. Kim, D. Ko, M.T. Smith, R.R. Hammond, P.C. Stair, K.R. Poeppelmeir, J. Catal. 223 (2004) 419–431.
[20] P. Moggi, M. Devillers, P. Ruiz, G. Predieri, D. Cauzzi, S. Morselli, O. Ligabue, Catal. Today 81 (2003) 77–85.
[21] A.V. Kucherov, A.V. Ivanov, T.N. Kucherova, V.D. Nissenbaum, L.M. Kustov, Catal. Today 81 (2003) 297–305.
[22] M. Sarzi-Amadè, S. Morselli, P. Moggi, A. Maione, P. Ruiz, M. Devillers, Appl. Catal. A: Gen. 284 (2005) 11–20.
[23] A. Galli, J.M. López Nieto, A. Dejoz, M.I. Vazquez, Catal. Lett. 34 (1995) 51–58.
[24] J.G. Eon, R. Olier, J.C. Volta, J. Catal. 145 (1994) 318–326.
[25] A. Corma, J.M. López Nieto, N. Paredes, Appl. Catal. A: Gen. 104 (1993) 161–174.
[26] C.M. Parler, J.A. Ritter, M.D. Amiridis, J. Non-Cryst. Solids 279 (2001) 119–125.
[27] A. Haoudi, P. Dhamelincourt, A. Mazzah, M. Drache, P. Conflant, Int. J. Inorg. Mater. 3 (2001) 357–366.
[28] M.D. Wildberger, T. Mallat, U. Göbel, A. Baiker, Appl. Catal. A: Gen. 168 (1998) 69–80.
[29] G. Bellussi, M.S. Rigutto, Stud. Surf. Sci. Catal. 85 (1994) 177–203.
[30] D.C.M. Dutoit, M. Schneider, P. Fabrizioli, A. Baiker, J. Mater. Chem. 7 (1997) 271–278.
[31] M. Baltes, K. Cassiers, P. Van Der Voort, B.M. Weckhuysen, R.A. Schoonheydt, E.F. Vansant, J. Catal. 197 (2001) 160–171.
[32] J. Chastain (Ed.), Handbook of X-Ray Photoelectron Spectroscopy, Perkin-Elmer Corporation, 1992.
[33] P. Van Der Voort, E.F. Vansant, Micropor. Mesopor. Mater. 38 (2000) 385–390.
[34] T. Kataoka, J.A. Dumesic, J. Catal. 112 (1988) 66–79.
[35] J.L.G. Fierro (Ed.), Spectroscopic Characterisation of Heterogeneus Catalyst, Catalysis and Surface Science Series, vol. 57, Elsevier, Amsterdam, 1990.
[36] J. Keränen, A. Auroux, S. Ek, L. Niinistö, Appl. Catal. A: Gen. 228 (2002) 213–225.
[37] C. Wang, R.G. Herman, C. Shi, Q. Sun, J.E. Roberts, Appl. Catal A: Gen. 247 (2003) 321–333.
[38] G. Connell, J.A. Dumesic, J. Catal. 105 (1987) 285–298.
[39] X. Gao, S.R. Bare, B.M. Weckhuysen, I.E. Wachs, J. Phys. Chem. B 102 (1998) 10842–10852.
[40] H. Dai, A.T. Bell, E. Iglesia, J. Catal. 221 (2004) 491–499.
[41] E. Heracleous, M. Machli, A.A. Lemonidou, I.A. Vasalos, J. Mol. Catal. A: Chem. 232 (2005) 29–39.
[42] V. Murgia, E. Sham, J.C. Gottifredi, E.M. Farfán Torres, Latin Am. Appl. Res. 34 (2004) 75–82.